Importance of spin current generation and detection by spin injection and the spin Hall effect for lateral spin valve performance

A. Pfeiffer,[1,2] R. M. Reeve,[1,2] and M. Kläui[1,2,a)]
[1)] *Institut für Physik, Johannes Gutenberg-Universität Mainz, 55099 Mainz, Germany*
[2)] *Graduate School of Excellence Materials Science in Mainz (MAINZ), Staudinger Weg 9, 55128 Mainz, Deutschland*

(Dated: 7 September 2018)

Lateral spin valves are attractive device geometries where functional spin currents can be generated and detected by various mechanisms, such as spin injection and the direct and the inverse spin Hall effect. To understand the mechanisms behind these effects better, as well as their potential for application in devices, we combine multiple mechanisms in multi-terminal Pt-Py-Cu lateral spin valves: We generate pure spin currents in the copper spin conduit both via the spin Hall effect in platinum and electric spin injection from permalloy and detect signals both via conventional non-local detection and via the inverse spin Hall effect in the same device at variable temperatures. Differences are observed, which we explain by the different spin injection and detection mechanisms, revealing their importance for the temperature dependence, which is not just governed by the spin transport in the conduit as previously claimed. By determining a different sensitivity of the observed effects on the interfaces, we highlight the importance of the exact current path for the device operation.

PACS numbers: Valid PACS appear here
Keywords: Suggested keywords

I. INTRODUCTION

The lateral spin valve geometry allows for a convenient and effective way to generate pure diffusive spin currents with reduced heating and Oersted fields at the position of a manipulated spin state.[1–3] Usually, these devices consist of two sub-micron ferromagnetic (FM) electrodes which are spatially separated, but connected via a non-magnetic (NM) spin conduit, such as a metal with low spin orbit coupling and low resistivity like Cu or[4] Al[5], or alternatively a semiconductor or graphene.[6] By applying a spin polarized charge current from the first ferromagnet, the injector, through the FM/NM interface, a spin accumulation is generated at this interface and diffuses in the direction of the second ferromagnetic electrode, the detector. At the NM/FM interface, the spin accumulation is absorbed and applies a spin transfer torque on the local magnetization which can be employed e.g. to switch the magnetization[3] or to displace a magnetic domain wall efficiently.[7–9] Compared to the described conventional non-local spin injection, the spin Hall effect (SHE)[10,11] provides additional mechanisms to generate pure spin currents. In this case, a pure spin current is generated perpendicular to an applied charge current in non-magnetic materials with large spin orbit coupling, with intrinsic contributions in Platinum[12,13] and Tungsten[14] and extrinsic effects in heavy metal alloys such as CuBi[15,16], CuIr[17] and AuTa.[18] The reciprocal effect, the inverse spin Hall effect (iSHE)[4,19] converts a spin current back into a measurable charge current. Since the physical mechanisms underlying the different spin current injection and detection mechanisms are very different, it is to be expected that the adoption of a particular approach should have both a qualitative and quantitative impact on the properties and performance of a lateral spin valve. To check and understand this, one needs, however, to be able to study the influence of varying temperatures on the different mechanisms in one single device.

In literature, the temperature dependence of the conventional non-local signal has been extensively studied for different systems.[20–22] When reducing the temperature from room temperature, it is observed within a certain temperature range, that the spin signal shows a monotonic increase with decreasing temperature. This result can be well, at least qualitatively, explained by the Elliot-Yafet mechanism which connects the reduction in the resistivity of the NM with an increase of the spin diffusion length.[23] However, at low temperatures a non-monotonic behaviour is often seen with an explicit maximum and subsequent downturn of the signal, which is not reflected in the resistivity of the conduit and would therefore seem to contradict Elliot-Yafet theory. Various explanations have been put forward to explain the low temperature contribution, including potential increased surface scattering[22] as well as magnetic impurity scattering via a manifestation of the Kondo effect for impurities both at the interfaces of the device[21,24] and in the bulk of the conduit, depending on the fabrication method and purity of the source material.[25] Overall, such explanations of the temperature dependence of the signals are almost exclusively based on transport effects within the NM spin conduit. However, we recently demonstrated that this is not the whole picture, since on comparing thermally generated spin signals[26] with electrically based

[a)] Electronic mail: klaeui@uni-mainz.de

ones, significant differences in the temperature dependence were observed, demonstrating that the spin current generation mechanism also plays an important role.[27]

The most promising alternative spin current generation mechanism to spin injection that has also been employed in lateral spin valves is the spin Hall effect.[11] A variety of experiments have been performed in such systems employing the spin Hall effect to generate spin currents and the inverse spin Hall effect to detect them.[4,28] Additionally, spin Hall electrodes have been used as absorber materials between the two ferromagnetic electrodes of a conventional lateral spin valve geometry.[18,29] From such experiments it is possible to extract an effective spin Hall angle of the materials, with different temperature dependences observed in different cases, including findings that the spin Hall angle is weakly temperature dependent or even temperature independent.[4,18,28,29] It is predicted that the temperature dependence of the spin Hall effect should be strongly dependent on the underlying physical mechanisms at play, with different predicted behaviour for intrinsic and extrinsic contributions[30,31] as also demonstrated recently experimentally.[32] Furthermore it is often found that the sizes of the spin Hall angles derived from such non-local measurements are much smaller than those determined from other measurement schemes, such as spin pumping[33], spin Hall magnetoresistance measurements[34] or spin transfer torque ferromagnetic resonance.[35] Liu et al. could explain these small spin Hall angles by a significant shunting of the generated charge current due to the highly conductive and thick NM layer, requiring a numerical correction factor to be employed in the analysis.[36] Yan et al. were able to directly determine extraordinary large spin Hall effect based spin signals in graphene tunnel barrier samples, where the shunting is efficiently suppressed due to the high resistivity of the graphene.[6] For metallic systems, one way to determine the correct spin Hall angles automatically is to exploit 3D modelling, which takes into account the shunting of the generated charge current in the NM correctly.[16] Measurements have also been performed comparing spin current detection using conventional non-local detection in ferromagnets and the inverse spin Hall effect in heavy metals.[28–30] However, the employed geometries with parallel electrodes often entail severe drawbacks, since large hard axis external fields are required to set the correct injected spin direction, which is not practical for applications. What is not yet clear is whether the employment of the spin Hall effect to generate spin currents has a significant influence on the temperature dependent behaviour of the device performanence in comparison to conventional spin injection, similar to the case for thermally generated spin currents.[27] Furthermore, if the spin current injection mechanism is important for the temperature evolution, it is to be expected that the detection mechanism would play an equivalent role, assuming Onsager reciprocity holds. Yet this remains to be tested for metallic systems.

In this work we compare the role of different mechanisms for spin current detection and generation in lateral spin valve devices. We develop a special kinked geometry that is uniquely suited to control the system and simultaneously probe spin currents generated by spin injection and the spin Hall effect, as well as spin signal detection by both the inverse spin Hall effect and conventional non-local detection. We find a markedly different sensitivity of the iSHE and the conventional non-local signal on the measurement probe configuration, which we explain based on the importance of the current path within the device. We compare the temperature behaviour of the signals, finding differences between the different spin signals, which demonstrates that it is not only spin transport that plays a role but that spin injection and spin absorption mechanisms additionally govern the temperature dependence of the signals.

II. FABRICATION

Lateral spin valve samples with a kinked geometry as shown in the inset of Fig. 1 are fabricated on a sapphire substrate by electron beam lithography and lift-off techniques. In the first step, 100 nm wide and 10 μm long wires together with alignment markers are patterned and we deposited 12 nm of Pt using magnetron sputtering. In the second step, 100 nm and 150 nm wide and 15 μm long wires are patterned perpendicularly to the Pt wire and 35 nm of Py was deposited by UHV thermal evaporation. The different widths are chosen to assure that the Py wires have different switching fields, with the left Py wire 100 nm and the right Py wire 150 nm in width, resulting in a lower switching field for the right Py wire. In the last step, in situ argon milling is used to clean the interfaces of the Py wires and the Pt stripe before the 100 wide and 150 nm thick Cu bridge is deposited, together with electric contacts.

III. FIELD DEPENDENCE OF ISHE AND CONVENTIONAL NON-LOCAL SIGNAL

To measure the inverse spin Hall effect, an average alternating current of 1.4 mA with a frequency of 2221 Hz is applied between the top contact of the left Py wire (contact 4) and the Cu wire (contact 8). The iSHE-voltage, V_{iSHE}, is measured between the two ends of the Pt stripe (contact 2 and contact 3) and between the Cu bridge (contact 1) and the top end of the Pt stripe (contact 2) simultaneously with two lock-in amplifiers, as shown in the inset of Fig. 1a). We define the iSHE-resistance, R_{iSHE}, by dividing the measured voltage by the applied current. All hysteresis curves are shifted to 0 mΩ at 0 mT for a better comparison of the different plots.

To generate the iSHE-signal, an external magnetic field is swept between -150 mT and +150 mT parallel to the easy axes of the Py wires, as indicated in Fig. 1. Since

the generated charge current due to the iSHE is given by

$$J_{iSHE} \propto J_s \times \sigma, \tag{1}$$

the polarity of the generated charge current in the Pt, J_{iSHE}, changes sign by changing the orientation of the diffusive spin current, J_s. The magnetization orientation of the left Py wire switches by sweeping the external magnetic field, resulting in a switch of the orientation of the pure spin current in the Cu bridge. The iSHE-signal, as shown in Fig. 1a), therefore shows two levels which are connected to the magnetization switching of the Py wire and the resulting change in the injected spin current orientation, which is drawn as a green arrow above the plot. In previous publications, the SHE wires and the magnetic wires were often all oriented perpendicularly to the NM wire and the external field had to be swept perpendicular to the easy axes in order to generate the maximum iSHE signal, which prevents exact control of the magnetization direction. A major advantage of our device geometry is that we can connect the appearance of the iSHE signal with the switching of the magnetic wire along its easy axis and much lower external fields are required to generate the signal. Furthermore, the two states yielding the two different levels are stable at remanence, eliminating any field effects that complicate the interpretation. Additionally, we measure the iSHE signal not only between the two ends of the Pt stripe (contact 2 and contact 3), but also between the Cu bridge (contact 1) and one part of the Pt stripe (contact 2). These two signals are similar in size, while the signal measured between the bottom part of the Pt stripe (contact 3) and the Cu bridge (contact 1) is about 0.01 $m\Omega$ and not shown. The appearance of these iSHE signals between the Pt stripe and the Cu bridge is connected to the shunting of the generated charge current in the Pt by the thick and highly conductive Cu bridge. This phenomenon was previously accounted for theoretically by the implementation of a shunting factor, x, in the 1D diffusion model[13] or is automatically taken into account using 3D modelling[16] while it is here shown experimentally. If we check the quantitative size of the signals, we notice that the signal shown in red is the sum of the two other signals.

To measure the non-local signal, the same alternating current with the same frequency as in the iSHE case is applied between the Cu bridge (contact 1) and the top end of the left Py wire (contact 4). The non-local voltage, V_{NL}, is measured simultaneously with two lock-in amplifiers between the top part of the right Py wire (contact 6) and the Cu bridge (contact 8) and between the bottom part of the right Py wire (contact 7) and the Cu bridge (contact 8), as shown in the inset of Fig. 1b). As for the inverse spin Hall effect case, the measured voltage is divided by the applied current to define the non-local resistance, R_{NL}. To generate the non-local signal, an external magnetic field is applied, as before. As can be seen in Fig. 1b), the resulting conventional non-local signals look very different compared to the inverse spin Hall effect based ones. In the non-local case, we determine two jumps at positive fields, corresponding to the separate switching of the two Py wires. The different levels in the signal then correspond to either parallel or antiparallel alignment of the electrodes' magnetization. Starting with negative external magnetic fields, the pure spin current and the magnetization of the detector are aligned parallel and we determine a large non-local signal. At an external field of +50 mT, the magnetization of the detector switches. This switching leads to an antiparallel alignment between pure spin current and detector magnetization orientation, resulting in a low non-local signal. For an external magnetic field of +100 mT the left Py wire switches its magnetization (as also seen in the iSHE signal) and the pure spin current and magnetization orientation of the detector are parallel again and we measure the high non-local signal.

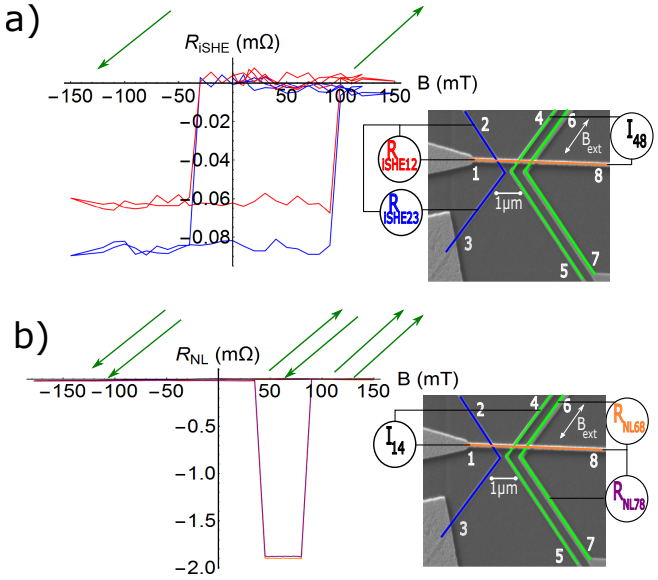

FIG. 1. Different signals as a function of applied external field measured at 4.2 K for current injection in Py 1 and detection in either a) Pt by the inverse spin Hall effect or b) Py 2 by conventional non-local detection. In both measurements, the external magnetic field is swept parallel to the easy axes of the Py wires.
a) iSHE based signal, with one jump at negative and one jump at positive external magnetic field, depending on the spin current orientation in the Cu bridge as drawn in green arrows above the hysteresis curve.
b) Conventional non-local detection with the spin states depending on the relative alignment of the pure spin current and the detector magnetization, schematically drawn as green arrows above the hysteresis curve.

The differences in the signals shown in Fig. 1a),b) reflect the differences in the underlying detection mechanisms. For the non-local signal, we probe the shift in the chemical potential of the Cu bridge and link the measured voltage change between high and low non-local signal to the number of spins absorbed at the interface and the signal is independent of the probe configuration. For the

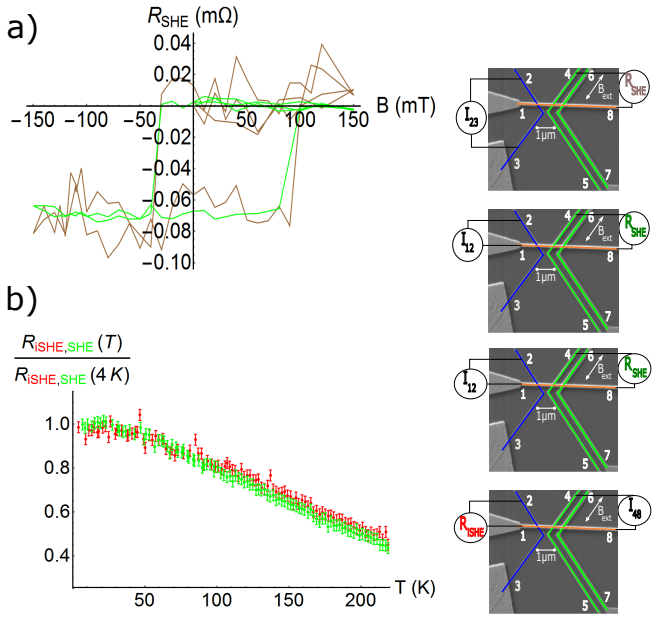

FIG. 2. a) Spin hall effect based hysteresis curves at 4.2 K with the measurement configuration as shown in the insets. A charge current is either applied completely through the Pt stripe (brown) or through the top part of the stripe and the Cu bridge (green).
b) Temperature dependence of the spin signal based on spin injection by the spin Hall effect (green) and of the inverse spin Hall effect based on conventional non-local spin injection (red) with the injection and detection configuration shown in the insets. The same temperature behaviour is observed as expected from the Onsager reciprocity.

inverse spin Hall effect, a charge current is generated in the Pt stripe due to spin dependent scattering and this charge current can be measured as an electric voltage. Due to shunting of the generated charge current in the Pt stripe by the Cu bridge, the measured voltage is significantly smaller and depends strongly on the exact current path at this interface and is therefore highly sensitive to the geometry and properties of the detector element, as well as the detection mechanism employed.

This means that in a lateral spin valve, different interfaces lead to quantitatively different spin signals and different detection schemes provide qualitatively different device behaviour. Devices based on the SHE show great promise, in particular based on recently developed materials with particular large spin Hall angles.[15–18] Such a sensitivity on the interface properties, however, could prove disadvantageous for device reliability, calling for robust schemes to prepare reliable interfaces in order to enable sufficiently robust operation for technology.

IV. RECIPROCITY BETWEEN SHE AND ISHE

To study the reciprocity between the iSHE and the SHE via the Onsager relation[4,37], charge current application and voltage detection are reversed as shown in Fig. 2a) for a temperature of 4.2 K. The charge current in these measurements is applied either completely through the Pt stripe (brown curve in Fig. 2a)) or between the top part of the Pt stripe and the Cu bridge (green curve in Fig. 2a)). In this situation, the flowing charge current in the Pt stripe leads to a spin current perpendicular to the charge current. This spin current enters the Pt/Cu interface with its orientation being parallel or antiparallel to the magnetization of the left Py wire, acting as the detector. Analogous to the non-local measurement, a high spin signal is observed for a parallel alignment between spin current and magnetization orientation, while for an antiparallel alignment a low spin signal is measured. As seen in previous publications, signals with the current flowing completely through the Pt stripe show a low signal to noise ratio, so it can be difficult to determine the SHE signal properly.[6] However, it can be seen that the second probe configuration yields a comparable signal, yet with much less noise, making it an attractive alternative for both experiments and devices. Since noise becomes a larger issue at elevated temperatures when the signal decreases, we therefore use the second probe configuration to probe the temperature evolution. This is plotted, alongside the reciprocal iSHE signal following spin current generation via spin injection from Py, in Fig. 2b). The error bars are defined by

$$\Delta = \sqrt{\left(\frac{20\,\mathrm{nV}}{\sqrt{N_1}}\right)^2 + \left(\frac{20\,\mathrm{nV}}{\sqrt{N_2}}\right)^2}, \qquad (2)$$

where 20 nV is the noise level of the lock-in amplifier across the whole temperature range and $N_{1,2}$ are the number of data points for the high and low signal levels, which typically is around 50 in each case. Due to the employment of a 5000 Ω pre resistor before the sample, the charge current flowing through the low resistive wires is essentially constant as a function of temperature. As can be seen, the normalized signals in Fig. 2b) show the same temperature dependence, as expected from the Onsager reciprocity.

V. TEMPERATURE DEPENDENCE OF SIGNALS FOR THE DIFFERENT DETECTION METHODS

We now study the temperature dependence of the non-local signal and the inverse spin Hall effect signal, as shown in Fig. 3.

For a quantitative comparison the spin signals are normalized to the signal measured at 4.2 K. In the low temperature range between 4.2 K and 30 K, we find for both cases a constant signal. In the temperature range between 60 K and 300 K, we observe an approximately linear decrease of both signals with increasing temperature and with both signals having the same slope. However, in the intermediate temperature range, the two signals differ with an evident shift for the onset of the reduction

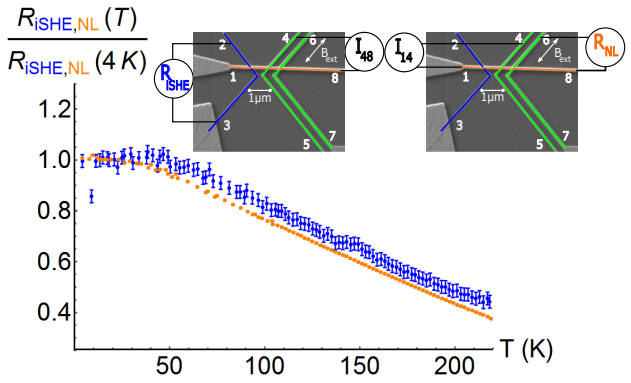

FIG. 3. Temperature dependence of the normalized non-local and the iSHE signal with the probe configurations shown in the insets. In the two cases the injection mechanism is the same while the detection method differs. Differences in the temperature behaviour are evident, revealing a contribution from the detection method in addition to the usually considered transport effects.

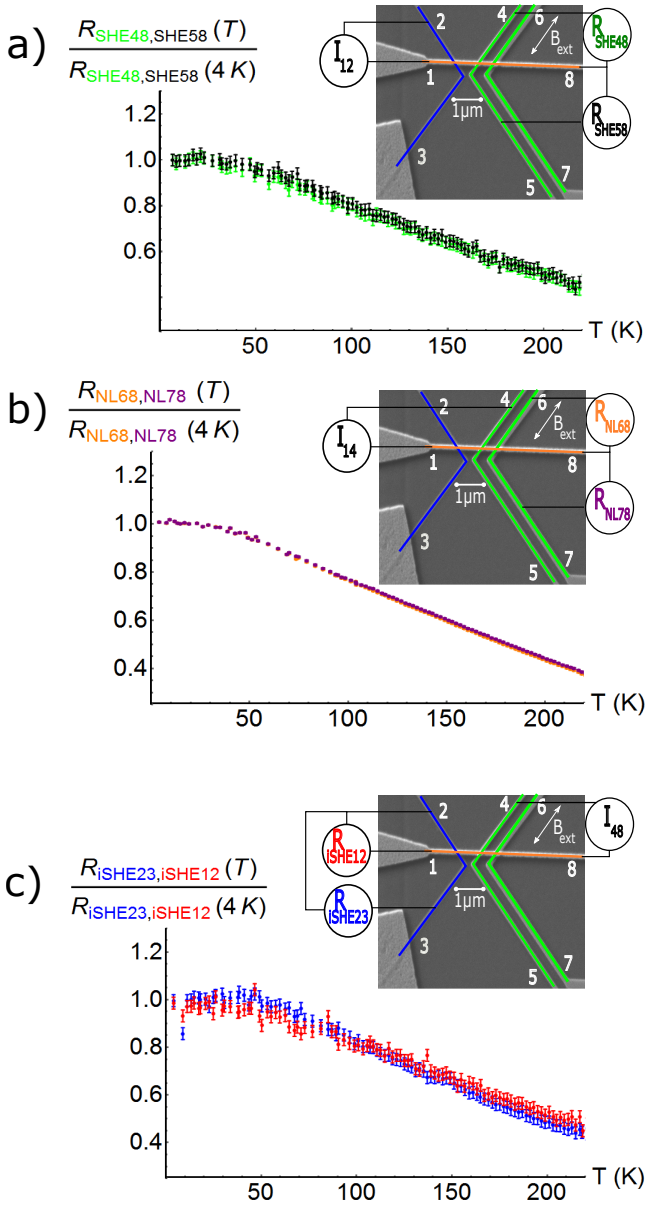

FIG. 4. Temperature dependence of the different effects for different injection and detection probe configurations.
a) Temperature dependence of two normalized spin Hall effect based spin signals measured on either side of the conduit.
b) Temperature dependence of the two normalized non-local signals, measured on either side of the conduit.
c) Temperature dependence of two normalized inverse spin Hall effect based spin signals with the signal either measured to one side of the Pt stripe (red) or across the whole length of the Pt (blue).

of the iSHE signal. In previous publications, the temperature dependence of both the non-local signal[21,22,27,38] and the iSHE signal[13,16] have been separately studied in metallic spin valve systems. For the non-local case, similar signals as the one shown here were found, where the signal behaviour in the high temperature range between 60 K and 300 K is usually explained based on Elliot-Yafet theory.[23] In this model, the decrease of the resistivity with a decrease of temperature leads to a reduction of spin scattering in the nonmagnetic channel during the spin transport. This increase of the spin diffusion length increases the number of spins reaching the NM/FM interface and therefore the signal is increased. A variety of explanations have been put forward to explain the low temperature regime for the non-local signal as discussed in the introduction.

Strikingly, however, most explanations of the temperature behaviour of the signals are only based on spin current *transport* phenomena[20–25] within the conduit and ignore effects of the generation and detection mechanisms. Our previous work shows that the spin current *generation* mechanism also plays a role.[27] Here we now see clearly that there is an additional influence of the spin current *detection* mechanism.

We now analyze the temperature dependence further. For the temperature dependence of the (inverse) spin Hall effect, Yan et. al measured tunnel contact based graphene spin valves and found a strong decrease of the iSHE signal with decreasing temperature.[6] In our measurements, we determine a completely different behaviour with an increase of the iSHE signal with decreasing temperature, indicating that different physical effects are relevant for the metallic spin valves studied here as compared to the previous tunnel contact based ones. A number of different factors need to be considered when describing the influence of temperature on the signals. In our case, the general trend in both cases can be explained based on the temperature evolution of the spin diffusion length in the conduit. While the exact values depend crucially on the purity and growth of the material, the spin diffusion length in Cu has been extensively studied as a function of temperature with typical values changing by almost 100 % from around 500 nm at 300 K to 900 nm

at 4 K.[4,27] This is reflected in the strong increase in both signals for lower temperatures as observed here. However since the same conduit is used in each case, such transport effects can not account for the differences we see. Another possible contribution to the signal is thermal spin currents due to the spin dependent Seebeck or spin Seebeck effect. In our samples the main heating effect is expected to arise at the injection Py/Cu interface, which is the same for both measurements. To quantify such potential contributions we attempted to measure the thermal spin current in the second harmonic signal.[27] However, we could not detect a signal within the noise level of our apparatus, which we attribute to low heating from the low resistive interfaces, confirming that such contributions are negligible in this work.

We now focus on the most prominent contributing factors which are different for the two detection schemes. For the conventional non-local scheme at the Py wire, standard 1D models can be used to describe the dependence of the signal on the spin polarization and spin diffusion of the magnetic material[39] as well as the interface resistivity.[40] In particular for Py, previous studies including our own work find that the spin polarization of Py is only weakly temperature dependent in the temperature range we probe here, which can be explained by the Curie temperature of permalloy of around 850 K.[4,22,38]. More recently temperature dependent contributions from Kondo magnetic impurity scattering in the Cu in the vicinity of interface as a result of interdiffusion have also been identified[24,25] which could suppress the detection for the Py/Cu interface even up to room temperature[21] but which would not be expected for the Pt/Cu interface. However, in previous results, the size of such signal suppression was strongly temperature dependent in the here studied temperature range, since the effect only emerges around the Kondo temperature of the system. We observe an essentially constant offset between the signals above 60 K and hence we do not expect this to be the origin of the differences. For the detection by the iSHE at the Pt stripe, one important factor is the spin Hall angle. Indeed, for tunnel-barrier based spin valves with graphene conduits this was found to dominate the temperature dependence of the signal as a consequence of the temperature independent graphene spin diffusion length.[6] As a result, the decrease of the Pt resistivity and correlated decrease in the spin Hall angle[13] led to a decrease of the spin signal. In our samples we measure a change in resistivity of the Pt from 61 $\mu\Omega cm$ at 300 K to 36 $\mu\Omega cm$ at 4 K which would only lead to small changes of the spin Hall angle of around 1 %[28,29,34], which are not sufficient to qualitatively explain the device behaviour, unlike the tunnel-barrier case and which are smaller than the effect we observe here. Finally, as already demonstrated, the effect of current shunting at the Pt electrode is of vital importance for the size of the iSHE signal and this too will be strongly temperature dependent due to the changing resistivity ratio between Cu and Pt. Here we measure a change of the Cu resistivity from 4 $\mu\Omega cm$ at room temperature to 2 $\mu\Omega cm$ at 4 K and hence the shunting effect is more important at low temperature. The resulting ratio of Cu/Pt resistivity changes by over 15 % which is about the order of the size of the effect we observe here.

VI. INFLUENCE OF DETECTION PROBE CONFIGURATION

To get more information concerning the temperature dependent contributions of the different interfaces and gain deeper insight into the possible spin current absorption hotspots we performed further temperature dependent measurements where we probe different detection configurations for the three categories of measurement scheme, as shown in Fig. 4. For the case of conventional non-local injection/detection and spin Hall effect based signals where conventional non-local detection is also employed we find no difference depending on which interface is probed. This confirms our previous conclusions regarding the robustness of the conventional non-local detection scheme. For the inverse spin Hall effect based signals, however, differences are seen, depending on whether the whole Cu/Pt interface is probed or just one side. This result strongly suggests that the difference in signals observed in Fig. 3 is due to effects at the Pt/Cu interface, where the temperature dependence of the interface modifies potential current injection hotspots and changes the current paths in the device for inverse spin Hall effect detection. This provides an additional temperature dependent contribution to the signal for the generated iSHE current. In contrast, since conventional non-local detection is based on a generated voltage from chemical potential differences at the detector, the temperature dependence of the interface properties are less critical for the signal. Overall, the measurements show that the temperature dependence is mainly governed by the spin transport. Yet, there are modest differences between the (inverse) spin Hall signals and the conventional non-local signal, demonstrating that not only spin transport but also spin current generation and detection mechanisms have to be taken into account.

In summary, we studied multi-terminal Pt-Py-Cu based lateral spin valves with a special kinked geometry. This geometry allows us to connect the switching of the magnetization of the Py wires with the spin Hall effect, the inverse spin Hall effect and the non-local signal in one single device allowing for direct comparability. The geometry also allows for the different magnetic states to be stable at remanence ruling out field effects and this situation is also more suitable for applications. For the SHE and the iSHE we find a signal depending on the probe configuration which can be explained by the significant shunting of the charge current in the Cu bridge. This dependence of the signal on the probe configuration demonstrates that in lateral spin valves the device behaviour crucially depends on the different interfaces

and wire geometries. We study the temperature dependence of the SHE, the iSHE and the non-local signals. While the SHE and the iSHE signals show equivalent behaviour as expected from Onsager reciprocity, differences are seen when comparing detection via the iSHE and standard non-local detection. These differences in the temperature dependent behaviour demonstrate in addition to the normally considered spin transport, both spin current generation and detection mechanisms have to be taken into account for a full description of the device.

ACKNOWLEDGMENTS

We acknowledge financial support of the SFB/TRR 173 Spin+X: spin in its collective environment funded by the Deutsche Forschungsgemeinschaft (DFG, German Research Foundation) Project No. 290396061/TRR173, as well as the Graduate School of Excellence Materials Science in Mainz (No. GSC266). A. Pfeiffer and M. Kläui would like to thank the participants of the Sendai-Lorraine-Mainz Workshop in Sendai, Japan, for fruitful discussions.

[1] F. J. Jedema, A. T. Filip, and B. J. van Wees, Nature **410**, 345–348 (2001).
[2] M. Johnson and R. H. Silsbee, Phys. Rev. B **37**, 5312–5325 (1988).
[3] T. Yang, T. Kimura, and Y. Otani, Nat. Phys. **4**, 851–854 (2008).
[4] T. Kimura, Y. Otani, T. Sato, S. Takahashi, and S. Maekawa, Phys. Rev. Lett. **98**, 156601 (2007).
[5] A. Pfeiffer, R. M. Reeve, M. Voto, W. Savero-Torres, L. Lopez-Diaz, and M. Kläui, J. Phys.: Condens. Matter **29**, 085802 (2017).
[6] W. Yan, E. Sagasta, M. Ribeiro, Y. Niimi, L. Hueso, and F. Casanova, Nat. Commun. **8** (2017).
[7] M. Kläui, C. A. F. Vaz, J. A. C. Bland, W. Wernsdorfer, G. Faini, E. Cambril, L. J. Heyderman, F. Nolting, and U. Rüdiger, Phys. Rev. Lett. **94**, 106601 (2005).
[8] D. Ilgaz, J. Nievendick, L. Heyne, D. Backes, J. Rhensius, T. A. Moore, M. A. Niño, A. Locatelli, T. O. Menteş, A. v. Schmidsfeld, A. v. Bieren, S. Krzyk, L. J. Heyderman, and M. Kläui, Phys. Rev. Lett. **105**, 076601 (2010).
[9] N. Motzko, B. Burkhardt, N. Richter, R. Reeve, P. Laczkowski, W. Savero Torres, L. Vila, J.-P. Attané, and M. Kläui, Phys. Rev. B **88**, 214405 (2013).
[10] S. O. Valenzuela and M. Tinkham, Nature **442**, 176–179 (2006).
[11] J. Sinova, S. O. Valenzuela, J. Wunderlich, C. H. Back, and T. Jungwirth, Rev. Mod. Phys. **87**, 1213–1260 (2015).
[12] M.-H. Nguyen, D. C. Ralph, and R. A. Buhrman, Phys. Rev. Lett. **116**, 126601 (2016).
[13] E. Sagasta, Y. Omori, M. Isasa, M. Gradhand, L. E. Hueso, Y. Niimi, Y. Otani, and F. Casanova, Phys. Rev. B **94**, 060412 (2016).
[14] C.-F. Pai, L. Liu, Y. Li, H. W. Tseng, D. C. Ralph, and R. A. Buhrman, Appl. Phys. Lett. **101**, 122404 (2012).
[15] Y. Niimi, Y. Kawanishi, D. H. Wei, C. Deranlot, H. X. Yang, M. Chshiev, T. Valet, A. Fert, and Y. Otani, Phys. Rev. Lett. **109**, 156602 (2012).
[16] Y. Niimi, H. Suzuki, Y. Kawanishi, Y. Omori, T. Valet, A. Fert, and Y. Otani, Phys. Rev. B **89**, 054401 (2014).
[17] J. Cramer, T. Seifert, A. Kronenberg, F. Fuhrmann, G. Jakob, M. Jourdan, T. Kampfrath, and M. Kläui, Nano Lett. **18**, 1064–1069 (2017).
[18] P. Laczkowski, Y. Fu, H. Yang, J.-C. Rojas-Sánchez, P. Noel, V. T. Pham, G. Zahnd, C. Deranlot, S. Collin, C. Bouard, P. Warin, V. Maurel, M. Chshiev, A. Marty, J.-P. Attané, A. Fert, H. Jaffrès, L. Vila, and J.-M. George, Phys. Rev. B **96**, 140405 (2017).
[19] E. Saitoh, M. Ueda, H. Miyajima, and G. Tatara, Appl. Phys. Lett. **88**, 172509 (2006).
[20] T. Kimura, T. Sato, and Y. Otani, Phys. Rev. Lett. **100**, 066602 (2008).
[21] L. O'Brien, M. J. Erickson, D. Spivak, H. Ambaye, R. J. Goyette, V. Lauter, P. A. Crowel, and C. Leighton, Nat. Commun. **5**, 3927 (2014).
[22] E. Villamor, M. Isasa, L. E. Hueso, and F. Casanova, Phys. Rev. B **87**, 094417 (2013).
[23] R. J. Elliot, Phys. Rev. **96**, 266–279 (1954).
[24] K.-W. Kim, L. O'Brien, P. A. Crowell, C. Leighton, and M. D. Stiles, Phys. Rev. B **95**, 104404 (2017).
[25] J. T. Batley, M. C. Rosamond, M. Ali, E. H. Linfield, G. Burnell, and B. J. Hickey, Phys. Rev. B **92**, 220420 (2015).
[26] A. Schlachter, J. L. Bakker, J.-P. Adam, and B. J. van Wees, Nat. Phys. **6**, 879–882 (2010).
[27] A. Pfeiffer, S. Hu, R. M. Reeve, A. Kronenberg, M. Jourdan, T. Kimura, and M. Kläui, Appl. Phys. Lett. **107**, 082401 (2015).
[28] L. Vila, T. Kimura, and Y. Otani, Phys. Rev. Lett. **99**, 226604 (2007).
[29] M. Isasa, E. Villamor, L. E. Hueso, M. Gradhand, and F. Casanova, Phys. Rev. B **91**, 024402 (2015).
[30] T. Kimura, Y. Otani, and L. Vila, J. Appl. Phys. **103**, 07F310 (2008).
[31] C. Gorini, U. Eckern, and R. Raimondi, Phys. Rev. Lett. **115**, 076602 (2015).
[32] G. V. Karnad, C. Gorini, K. Lee, T. Schulz, R. Lo Conte, A. W. J. Wells, D.-S. Han, K. Shahbazi, J.-S. Kim, T. A. Moore, H. J. M. Swagten, U. Eckern, R. Raimondi, and M. Kläui, Phys. Rev. B **97**, 100405 (2018).
[33] M. Obstbaum, M. Härtinger, H. G. Bauer, T. Meier, F. Swientek, C. H. Back, and G. Woltersdorf, Phys. Rev. B **89**, 060407 (2014).
[34] S. R. Marmion, M. Ali, M. McLaren, D. A. Williams, and B. J. Hickey, Phys. Rev. B **89**, 220404 (2014).
[35] L. Liu, T. Moriyama, D. C. Ralph, and R. A. Buhrman, Phys. Rev. Lett. **106**, 036601 (2011).
[36] L. Liu, R. A. Burman, and D. C. Ralph, arXiv:1111.3702 (2012).
[37] P. Jacquod, R. S. Whitney, J. Meair, and M. Büttiker, Phys. Rev. B **86**, 155118 (2012).
[38] N. Motzko, N. Richter, B. Burkhardt, R. Reeve, P. Laczkowski, L. Vila, J. Attané, and M. Kläui, Phys. Status Solidi A **211**, 986–990 (2014).
[39] E. Sagasta, Y. Omori, M. Isasa, Y. Otani, L. E. Hueso, and F. Casanova, Appl. Phys. Lett. **111**, 082407 (2017).
[40] S. Takahashi and S. Maekawa, Phys. Rev. B **67**, 052409 (2003).